Soil microbial habitats in an extreme desert Mars-analogue environment

Kimberley A. Warren-Rhodes[1,2+#], Kevin C. Lee[3+], Stephen D.J. Archer[3], Donnabella C. Lacap-Bugler[3], Linda Ng Boyle[4], David Wettergreen[5], Kris Zacny[6], Cecilia Demargasso[7], Jeff Moersch[8], Guillermo Chong[7], Srinivasan Vijayarangan[5], Cinthya Tebes[7], Michael Wagner[5], Ken Tanaka[9], Trent Hare[9], Christopher Gayle Tate[8], Alian Wang[10], Jie Wei[10], Greydon Foil[5], Nathalie Cabrol[1,2], and Stephen B. Pointing[11#]

[1] *NASA Ames Research Center, Moffett Field, CA, USA.*

[2] *The SETI Institute, Mountain View, CA, USA*

[3] *School of Sciences, Auckland University of Technology, Auckland, New Zealand.*

[4] *College of Engineering, University of Washington, Seattle, WA, USA*

[5] *Institute of Robotics, Carnegie-Mellon University, Pittsburgh, PA, USA*

[6] *Honeybee Robotics and Spacecraft Mechanisms Corp, Pasadena, CA, USA*

[7] *Universidad Católica del Norte, Antofagasta, Chile*

[8] *Department of Earth and Planetary Science, University of Tennessee, Knoxville, TN, USA*

[9] *United States Geological Survey, Flagstaff, AZ, USA*

[10] *Department of Chemistry, Washington University, St. Louis, OH, USA*

[11] *Division of Science, Yale-NUS College, National University of Singapore, Singapore*

[+] These authors contributed equally

[#] Email: K.A.W-R. krhodes@seti.org or S.B.P. stephen.pointing@yale-nus.edu.sg

Summary

The Atacama Desert represents one of the closest terrestrial analogues to Mars' surface and subsurface environments. Understanding the distribution and drivers of life in the soil may thus give critical clues on how to search for biosignatures in the Martian regolith with the upcoming Mars2020 and ExoMars missions. Here, we show the result of a field experiment that combined an autonomous rover-mounted drill with ground-truth from manual sample recovery to characterize the most extreme Atacama Desert soil habitats. Distinct habitability zones were identified in soil horizons to 800mm depth in two Mars-like terrains, an evaporite-rich playa and a gravel desert pavement. Highly specialised bacterial community assembly was depth-dependent and strongly influenced by soil geochemistry linked to moisture. Colonisation was also patchy and several putatively lifeless zones that correlated with high salt content were encountered. We demonstrate a clear linkage between geochemistry, moisture and biocomplexity in Mars analogue soils, and resident bacterial communities displayed putative traits that might allow survival in the Martian regolith. We discuss implication of the findings in extreme desert geobiological systems and their scientific and operational significance for upcoming Mars missions.

Introduction

The surface of Mars is dry, cold, and exposed to high levels of ionising radiation. However, data accumulated over the past decades by orbital and landed missions have demonstrated that early in its history the planet was habitable for life as we

know it. Sources of energy, carbon, nutrients, and shelters were abundant[1]. Mars supported surface and subsurface water and may still do in some circumstances, as well as organic molecules required for life[2]. As a result, Mars 2020 and ExoMars missions will be searching for biosignatures[3,4], and the investigation of terrestrial analogues can provide critical insights for the development of exploration strategies.

Among those, the hyper-arid core of the Atacama Desert in Chile is widely regarded as a tractable Mars analogue. The Atacama is the driest desert region on Earth [5] with precipitation events that are stochastic in nature and moisture inputs are extremely low [6]. The region has a long history of climatic stability as an extreme desert [7,8], resulting in the build-up of evaporates resembling those on Mars [6,9] at or near the arid limit for soil formation [10]. Animal and plant life are scarce in extreme deserts and instead surface microbial communities in mineral refugia and soil assume the dominant ecological role and are well-charatecrised[11]. Generally, patchy distribution of cyanobacteria-dominated refuge communities occur as surface features beneath quartz pebbles in desert pavement[12–14] and within deliquescent halite substrates [15–17].

Evidence for microbial colonisation in hyper-arid soils is scarce and contradictory (Online Supplementary Material, Table S1). Few viable bacteria have been recovered from Atacama soils and challenging environmental conditions have been postulated to preclude recovery of microbial biosignatures such as DNA[9], although a recent high-throughput sequencing study of near-surface soil indicated bacterial DNA biosignatures dominated by the phylum Actinobacteria were

recoverable[18]. Major geobiological knowledge gaps persist, and importantly the question of how microbial diversity may vary spatially in different terrain and within soil depth horizons in a Mars analogue. This is critical in the effort to build a clear picture of habitability in extreme deserts as well as informing the most appropriate depth at which to search for life on Mars [19].

To document these questions and support the development of biosignature exploration strategies, the NASA-funded *Subsurface Life in the Atacama Project* deployed a rover-mounted robotic drill to conduct sampling of soil geochemistry and biology in vertical soil horizon transects from the surface to 800mm depth. Manual sampling from soil pits was performed in parallel to ground-truth results and build a high-resolution picture of microbial community variation with terrain, habitat, location and depth.

The rover accessed soil samples along a 50km transect in a realistic simulation of Martian drilling operations within the hyper-arid core of the Atacama (Online Supplementary Material, Fig. S1). The field experiment took place over a period of two weeks in terrain units including desert pavement and playa, which revealed distinct soil geochemical profiles. Manually excavated soil pits were used to sample horizontally into undisturbed soil horizons for ground-truth. Using this approach, detailed geochemical and microclimate data for soil horizons were obtained to a depth of 800mm, as well as aseptic recovery of 85 samples for bacterial community estimation using molecular genetic biosignatures.

Extreme habitats in Atacama soil horizons

For both soil types a clear depth-dependent pattern in geochemistry was observed (Fig. 1, Online Supplementary Material, Fig. S2 and Table S3). Surface soils were strongly associated with elevated phosphorous levels in both playa and pavement units (Fig. 1). Desert pavement soils separated mainly due to pH and K, whilst playa soils displayed elevated levels of minerals linked to deliquescent evaporates and electrical conductivity (Fig. 1). Both desert pavement and playa subsurface soils displayed increasingly elevated (albeit very low) total carbon with depth (Fig. 1). The on-board rover instrumentation (Mars Microbeam Raman Spectrometer) corroborated these results[20], supporting our delineations of surface and terrain-specific subsurface soil geochemistry, plus gypsum, anhydrite and soluble salts geochemistry closely linked to moisture availability in playa soil.

Moisture values in the playa were consistently higher (approximately 4- to 20-fold) at all depths than those in the desert pavement soils (Online Supplementary Table S2). Soil moisture trends also broadly suggested the existence of depth groupings into distinct 'moisture zones' for both terrains into (a) a surface zone consisting of the top 100mm, where water availability is typically lowest, except in the short-term following a rain event; (b) a near-surface zone (100-500mm), where water availability peaks and persists after a rain event, with the particular depth of maximum moisture varying by the event size and soil mineralogy; and (c) a deep subsurface zone (≥500-800mm), where water availability is typically lowest and, most notably for the desert pavement soils, appeared to be un-impacted by large stochastic rainfall events (Online Supplementary Fig. S3).

Depth-defined microbial communities

Recoverable levels of environmental DNA were obtained for 29% of soil samples (n=25) and were at the limit for currently available quantification methods (0.067-6.5 ng/g soil, Online Supplementary Material Table S4)[21]. This highlights the stochastic and low biomass pattern of microbial colonisation in the most extreme desert soils where micro-habitat conditions are at or near the limit for life[6,9,11,22,23]. Linear Discrimination Analysis was employed to show that variables most strongly associated with soils where environmental DNA was irrecoverable ("lifeless soils") were sulphate sulphur (p = 0.001), depth (p = 0.003), electrical conductivity (p = 0.006), soluble salts (p = 0.006), cation exchange capacity (p = 0.007), magnesium (p = 0.008) (Online Supplementary Table S3). We also demonstrated that soil itself was not inhibitory to DNA recovery by successful extraction of DNA from playa and pavement soil "spiked" with bacterial cell suspensions (Online Supplementary Material). We therefore postulate that moisture bio-availability as determined by substrate chemistry and soluble salts may be a limiting factor to colonisation in extreme desert soils. Our DNA recovery rate was consistent with our expectations for the driest desert location on Earth and, in comparison with recovery rates for other less extreme desert locations [24]. It is worth noting that Antarctic mineral soils, another frequently used Mars analogue, appear to generally yield higher recovery rates, e.g.[25,26], but this is likely due to the less extreme nature of the growing season in Antarctic desert where long periods of frozen hibernation are punctuated by periods of moisture sufficiency [27].

Colonised soil displayed a clear negative correlation between microbial diversity and depth regardless of terrain type (Fig. 2a). Bacteria formed six diversity clusters that correlated with clearly defined depth ranges (and associated geochemistry/moisture zones) in the soil horizon (Fig. 3a). Ordinations of Bray-Curtis Similarity Index for bacterial communities revealed that whilst overall the desert pavement and playa had distinct community groupings, these overlapped considerably and particularly for surface communities (Online Supplementary Fig. S4). Sub-surface communities were more distinct between habitat types but also more heterogenous overall, due largely to the lower bacterial diversity within these soil micro-habitats. In all cases the drill samples showed a generally similar (although less pronounced) pattern in depth profile and diversity clusters that we attributed to mixing during recovery using the "bite" drill approach that can result in some vertical mixing of drill tailings (Figs. 2b & 3b).

To further unravel the influence of soil environment on bacterial diversity, we performed canonical correspondence analysis (CCA) to establish the correlation of distinct geochemistry for desert pavement and playa samples on the assembly of bacterial communities (Fig. 1). Bacterial diversity within the two soil habitats correlated with two groups of geochemical variables: The playa subsurface community was strongly correlated with 'salts', as indicated by electrical conductivity (EC), Ca/S (gypsum/anhydrite) and Mg/Na (likely halite). Conversely the pavement subsurface community associated with pH, total carbon and K. Another driver that appeared largely independent of these two groups was P and abundance for some commonly encountered surface bacterial taxa (e.g. B & C in Fig

1) appeared to be associated with this variable. The BEST multiple rank correlation routine was employed to further triangulate our data and rank the relative correlation of abiotic variables with the observed community assembly as follows: metal ions and phosphorous>sulphate sulphur>soluble salts>EC ($_pw$ = 0.595-0.609, p <0.05), and these observations broadly supported the ordinations and CCA analysis.

Highly specialised soil bacterial communities

The taxa we recovered from Atacama soil indicates a highly specialised bacterial community and this mirrors observations for other extreme desert soils [26,28,29] and the deep subsurface biosphere [30]. Bacterial taxonomic diversity appeared to be relatively more influenced by habitat in subsurface samples (desert pavement vs. playa) compared to a more cosmopolitan surface community (Fig. 4). Overall, communities were dominated by only three phyla: Actinobacteria, Alphaproteobacteria and Chloroflexi. The anoxygenic photoheterotrophic Chloroflexi displayed a pronounced pattern where surface communities were dominated by the "AKIW781" lineage of Chloroflexi, whereas subsurface Chloroflexi were less abundant and consisted mainly of an uncharacterised candidate class "Ellin6529" likely adapted to a non-phototrophic metabolism in the subsurface microhabitat. AKIW781 has also been recorded in desert varnish on rock surfaces [31] as well as a keystone taxon of hypolithic communities [13] in the Atacama. This indicates a cosmopolitan distribution and broad habitat preference among surface niches in this extreme desert. We speculate the gliding motility of chloroflexi may

confer an advantage via hydrotaxis in exposed surface niches[32], mirroring observations for cyanobacteria in semi-arid soil crusts[33] .

Overall the drill samples yielded weaker depth resolution but still corroborated observations from the manually collected 'groundtruth' samples (Fig. 4, Online Supplementary Material Fig. S5). Subsurface soil horizons were dominated by bacteria of the phylum Actinobacteria. At mid-depth ranges (100-300mm) pavement terrain communities largely comprised the orders Gaiellales (deep biosphere heterotrophic bacteria) and Nitriliruptorales (halo-alkalophilic nitrile-utilising bacteria) whereas playa samples were dominated by Euzebyales (unknown physiology). There were fewer deep soil samples from which to make comparisons, however the deeper communities (500-700mm) generally displayed lower taxonomic diversity and were dominated almost exclusively by a single facultative methylotrophic *Methylobacterium* taxon (Rhizobiales). Pavement horizons failed to yield biosignatures at depths below 500-630mmmm, whereas playa was habitable to the maximum drill depth of 800mm. This reflected long-term moisture availability in these depth horizons (Online Supplementary Material Fig. S3). The *Methylobacterium* found in deeper soil layers has also been isolated from African desert soil [34]. We speculate the C1 metabolism of this taxon allows it to exploit simple C1 compounds as well as sub-surface methane sources[35], also known to be released from subsurface sources on Mars [36].

This structuring of bacterial communities with soil depth towards highly specialised low diversity assemblages[37] is consistent with an observation for bacteria even at much deeper horizons hundreds of metres below the surface [38].

Other bacteria typically regarded as tolerant to desert surface conditions were not major components of the Atacama soil horizon communities. For example, subsurface soils displayed very low abundance putative spore-forming bacteria (11.7% overall OTUs), a complete absence of cyanobacterial taxa, and the highly desiccation-tolerant *Deinococcus*-Thermus group were represented by a single lineage of Trueperaceae candidate genus "B-42" recovered in just a few subsurface samples at low abundance (0.6 – 4.8%). This strongly suggests that a highly specialised community has been selected for by the distinct geochemistry and microclimate in the Mars analogue soils of the Atacama.

In the deepest and least-diverse communities multiple, albeit closely related, taxa occurred and this suggests that there may be a minimum level of biocomplexity that is required to sustain a desert soil community, and also reflects a low diversity reservoir from which recruitment may occur [39]. The absolute minimum may exist with multiple ecotypes of a single taxon, each adapted to exploit a given suite of microclimate and geochemical conditions [40]. They likely exhibit a strong preference for C1 and/or autotrophic taxa that are somewhat de-linked from their immediate surroundings in terms of carbon sequestration, and reflecting the extreme oligotrophic nature of these microhabitats.

Implications for detection of biosignatures on Mars

The autonomous rover drilling platform was able to yield soil samples that allowed combined resolution of soil geochemistry and microbial diversity at an unprecedented level of detail to depths of 800mm. The highly specialised but low-

diversity subsurface bacterial communities were encountered stochastically and displayed distinct depth-related zonation that was linked to moisture availability. It is not just a question of deeper is better as our data shows, but rather that a "sweet spot'" for habitability likely develops due to the complex interaction between geochemistry and water. Whilst the geochemistry of our analogue sites was similar to that of a putatively habitable Martian regolith[10], moisture in the Atacama is surface-sourced by fog and/or rain events [6], whereas on Mars subsurface sources may provide an upward migration of moisture similar to that observed in Antarctic mineral soil overlaying permafrost [41,42]. Thus, extrapolating a potential "sweet spot" for habitable subsurface locations on Mars would need to consider this along with the incident radiation regime and other Martian environmental variables.

The relevance of ecology and microbial habitats to past and possible extant life on Mars are finally coming to the fore in the robotic search for biosignatures on Mars[1]. Our results show that the interplay of soil geochemistry and water, as characterized by habitat type and microclimate zonation by depth is what strongly influences bacterial diversity and spatial distribution. The strong correlation with abiotic variables associated with moisture and salinity suggests that "following the water" is only part of the biosignature exploration solution in the search for potential habitable refuges on Mars. Consideration of surface and subsurface micro-habitat variability in geochemistry, originating with and adapted to possible water availability zones or reservoirs may also be key.

Given the ancient evolutionary origins of desert bacteria [43] and the ability among microorganisms to tolerate ionising radiation [44,45], a subsurface habitat that

reduces ionising radiation exposure to tolerable levels yet also caches residual water reservoirs (e.g., playa sediments at depth, as shown in this study) might facilitate life on Mars or have created habitable subsurface oases as the planet's surface became increasingly inhospitable [46,47]. As our study suggests, detecting such life or its residual biosignatures may prove highly challenging, given that even in the most extreme deserts on Earth these refuge communities are extremely patchy in distribution and occur with low biomass (Warren-Rhodes et al. 2007; Pointing and Belnap, 2012). The highly specialised nature of these microbial communities suggests that communities may be viable comprising just a few closely related taxa, thus presenting potential opportunity for targeting biosignature technology towards bacterial groups/metabolites likely to be encountered.

The drill apparatus employed in this study has demonstrated that sub-surface soil biosignatures can be autonomously recovered, although precise depth delineation requires refinement with the currently favoured bite drill used in this study, plus evaluation of factors such as shear forces on sample recovery and biosignature integrity. Whilst genetic biosignatures such as DNA used in our study may not ultimately be the primary method employed to search for traces of life on Mars, they provide essential "proof of concept" that an incontrovertible biological signature and the likely range for geochemical variables in a habitable subsurface environment can be recovered from a Mars-like soil using an autonomous rover.

Methods

Methods, including statements of data availability and public database accession numbers and references, are available in the online version of this paper.

References

1. Cabrol, N. A. The Coevolution of Life and Environment on Mars: An Ecosystem Perspective on the Robotic Exploration of Biosignatures. *Astrobiology* **18,** 1–27 (2018).
2. Martin-Torres, F. J. *et al.* Transient liquid water and water activity at Gale crater on Mars. *Nat. Geosci.* **8,** 357–361 (2015).
3. Farley, K. & Williford, K. Seeking Signs of Life and More: NASA's Mars 2020 Mission. *Eos (Washington. DC).* **98,** https://doi.org/10.1029/2017EO066153 (2017).
4. Vago, J. L. *et al.* Habitability on Early Mars and the Search for Biosignatures with the ExoMars Rover. *Astrobiology* **17,** 471–510 (2017).
5. Peel, M. C. & Finlayson, B. L. Updated world map of the Köppen-Geiger climate classification. *Hydrol. Earth Syst. Sci.* **11,** 1633–1644 (2007).
6. McKay, C. P. *et al.* Temperature and Moisture Conditions for Life in the Extreme Arid Region of the Atacama Desert: Four Years of Observations Including the El Nino of 1997. *Astrobiology* **3,** 393–406 (2003).
7. Clarke, J. D. A. Antiquity of aridity in the Chilean Atacama Desert. *Geomorphology* **73,** 101–114 (2006).
8. Hartley, A. J., Chong, G., Houston, J. & Mather, A. E. 150 million years of climatic stability: evidence from the Atacama Desert, northern Chile. *J. Geol. Soc.*

London. **162,** 421–424 (2005).

9. Navarro-Gonzalez, R. *et al.* Mars-like soils in the Atacama Desert, Chile, and the dry limit of microbial life. *Science* **302,** 1018–1021 (2003).

10. Ewing, S. A. *et al.* A threshold in soil formation at Earth's arid–hyperarid transition. *Geochim. Cosmochim. Acta* **70,** 5293–5322 (2006).

11. Pointing, S. B. & Belnap, J. Microbial colonization and controls in dryland systems. *Nat. Rev. Microbiol.* **10,** 551–562 (2012).

12. Warren-Rhodes, K. A. *et al.* Hypolithic cyanobacteria, dry limit of photosynthesis, and microbial ecology in the hyperarid Atacama Desert. *Microb. Ecol.* **52,** 389–398 (2006).

13. Lacap, D. C., Warren-Rhodes, K. A., McKay, C. P. & Pointing, S. B. Cyanobacteria and chloroflexi-dominated hypolithic colonization of quartz at the hyper-arid core of the Atacama Desert, Chile. *Extremophiles* **15,** 31–8 (2011).

14. Azúa-Bustos, A. *et al.* Hypolithic Cyanobacteria Supported Mainly by Fog in the Coastal Range of the Atacama Desert. *Microb. Ecol.* **61,** 568–581 (2011).

15. Davila, A. F. *et al.* Facilitation of endolithic microbial survival in the hyperarid core of the Atacama Desert by mineral deliquescence. *J. Geophys. Res.* **113,** G01028 (2008).

16. Wierzchos, J., Ascaso, C. & McKay, C. P. Endolithic cyanobacteria in halite rocks from the hyperarid core of the Atacama Desert. *Astrobiology* **6,** 415–422 (2006).

17. de los Ríos, A. *et al.* Comparative analysis of the microbial communities inhabiting halite evaporites of the Atacama Desert. *Int. Microbiol.* **13,** 79–89

(2010).

18. Crits-Christoph, A. *et al.* Colonization patterns of soil microbial communities in the Atacama Desert. *Microbiome* **1,** 28 (2013).

19. Fairen, A. *et al.* Astrobiology through the Ages of Mars: The Study of Terrestrial Analogues to Understand the Habitability of Mars. *Astrobiology* **10,** 821–843 (2010).

20. Tripathi, B. M. *et al.* Autonomous soil analysis by the Mars Micro-beam Raman Spectrometer (MMRS) on-board a rover in the Atacama Desert: A terrestrial test for planetary exploration. *Eukaryot. Cell* **46,** 1287–1297 (2017).

21. Pointing, S. B., Fierer, N., Smith, G. J. D., Steinberg, P. D. & Wiedmann, M. Quantifying human impact on Earth's microbiome. *Nat. Microbiol.* **1,** 16145 (2016).

22. McKay, C. P. Requirements and limits for life in the context of exoplanets. *Proc. Natl. Acad. Sci. U.S.A.* **111,** 12628–33 (2014).

23. Azua-Bustos, A., Caro-Lara, L. & Vicuña, R. Discovery and microbial content of the driest site of the hyperarid Atacama Desert, Chile. *Environ. Microbiol. Rep.* **7,** 388–394 (2015).

24. Chan, Y. *et al.* Hypolithic microbial communities: between a rock and a hard place. *Environ. Microbiol.* **14,** 2272–2282 (2012).

25. Pointing, S. B. *et al.* Highly specialized microbial diversity in hyper-arid polar desert. *Proc. Natl. Acad. Sci. U.S.A.* **106,** 19964–19969 (2009).

26. Lee, C. K. *et al.* The Inter-Valley Soil Comparative Survey: the ecology of Dry Valley edaphic microbial communities. *ISME J.* **6,** 1046–1057 (2012).

27. Pointing, S. B. *et al.* Biogeography of photoautotrophs in the high polar biome. *Front. Plant Sci.* **6,** (2015).

28. Chanal, A. *et al.* The desert of Tataouine: an extreme environment that hosts a wide diversity of microorganisms and radiotolerant bacteria. *Env. Microbiol.* **8,** 514–525 (2006).

29. Stomeo, F. *et al.* Hypolithic and soil microbial community assembly along an aridity gradient in the Namib Desert. *Extremophiles* **17,** 329–337 (2013).

30. Lau, M. C. Y. *et al.* An oligotrophic deep-subsurface community dependent on syntrophy is dominated by sulfur-driven autotrophic denitrifiers. *Proc. Natl. Acad. Sci. U.S.A.* **113,** E7927–E7936 (2016).

31. Kuhlman, K. R., Venkat, P., La Duc, M. T., Kuhlman, G. M. & McKay, C. P. Evidence of a microbial community associated with rock varnish at Yungay, Atacama Desert, Chile. *J. Geophys. Res.* **113,** G04022 (2008).

32. Hanada, S. in *The Prokaryotes* 515–532 (Springer Berlin Heidelberg, 2014).

33. Pringault, O. & Garcia-Pichel, F. Hydrotaxis of cyanobacteria in desert crusts. *Microb. Ecol.* **47,** 366–373 (2004).

34. Veyisoglu, A. *et al.* Methylobacterium tarhaniae sp. nov., isolated from arid soil. *Int. J. Syst. Evol. Microbiol.* **63,** 2823–2828 (2013).

35. Kao, Y. *et al.* Scale-dependent key drivers controlling methane oxidation potential in Chinese grassland soils. *Soil Biol. Biochem.* **111,** 104–114 (2017).

36. Stevens, A. H., Patel, M. R. & Lewis, S. R. Modelled isotopic fractionation and transient diffusive release of methane from potential subsurface sources on Mars. *Icarus* **281,** 240–247 (2017).

37. Delgado-Baquerizo, M. *et al.* A global atlas of the dominant bacteria found in soil. *Science* **359,** 320–325 (2018).

38. Rempfert, K. R. *et al.* Geological and geochemical controls on subsurface microbial life in the Samail Ophiolite, Oman. *Front. Microbiol.* **8,** 56 (2017).

39. Curtis, T. P. & Sloan, W. T. Prokaryotic diversity and its limits: microbial community structure in nature and implications for microbial ecology. *Curr. Opin. Microbiol.* **7,** 221–226 (2004).

40. Koeppel, A. *et al.* Identifying the fundamental units of bacterial diversity: a paradigm shift to incorporate ecology into bacterial systematics. *Proc. Natl. Acad. Sci. U.S.A.* **105,** 2504–9 (2008).

41. Goordial, J. *et al.* Nearing the cold-arid limits of microbial life in permafrost of an upper dry valley, Antarctica. *ISME J.* **10,** 1613–1624 (2016).

42. Stomeo, F. *et al.* Abiotic factors influence microbial diversity in permanently cold soil horizons of a maritime-associated Antarctic Dry Valley. *FEMS Microbiol. Ecol.* **82**, 326-340 (2012). doi:10.1111/j.1574-6941.2012.01360.x

43. Bahl, J. *et al.* Ancient origins determine global biogeography of hot and cold desert cyanobacteria. *Nat. Commun.* **2,** 163 (2011).

44. Pointing, S. B., Gareth Jones, E. B. & Jones, M. A. Radiosensitivity of fungi isolated from waterlogged archaeological wood. *Mycoscience* **37,** 455–458 (1996).

45. Sancho, L. G. *et al.* Lichens Survive in Space: Results from the 2005 LICHENS Experiment. *Astrobiology* **7,** 443–454 (2007).

46. O'Malley-James, J. T., Greaves, J. S., Raven, J. A. & Cockell, C. S. Swansong

biospheres: refuges for life and novel microbial biospheres on terrestrial planets near the end of their habitable lifetimes. *Int. J. Astrobiol.* **12,** 99–112 (2013).

47. Wadsworth, J. & Cockell, C. S. Perchlorates on Mars enhance the bacteriocidal effects of UV light. *Sci. Rep.* **7,** 4662 (2017).

Acknowledgements

The work was completed with funding from NASA Astrobiology Science and Technology for Exploring Planets (ASTEP) Program Grant NNX11AJ87G. The authors are grateful to Professor S. Craig Cary (University of Waikato) for assistance with biosecurity compliance and sample custody.

Author contributions

K.A.W-R., N.C. and S.B.P. conceived the study; D.W., K.Z., S.V., M.W. and G.F. built and operated the rover; K.A.W-R.; C.D., J.M., G.C., C.T., K.T., T.H., C.G.T., A.W. and J.W. conducted field operations and sampling; K.C.L., S.D.J.A., D.C.L-B. and S.B.P. processed soil samples and conducted geochemical analysis; S.D.J.A. and K.C.L. conducted molecular biology experiments; K.A.W-R, K.C.L., S.D.J.A., D.C.L-B, L.N-B. and S.B.P. performed data analysis; K.A.W-R., N.C. and S.B.P. wrote the manuscript.

Materials & Correspondence

Correspondence and requests for materials should be addressed to K.A.W-R Email: krhodes@seti.org or S.B.P. Email: stephen.pointing@yale-nus.edu.sg

Figure legends

Figure 1. Canonical Correspondence Analysis (CCA) triplot with symmetrical scaling indicating differences in soil geochemistry with terrain and depth, and influence of these abiotic variables on bacterial communities and individual taxa. The three most abundant taxa are labelled (A, B, C). The circle size of each sample indicates Chao1 species richness index of the respective community.

Figure 2. Shannon's Diversity estimates (H) for bacterial diversity in vertical soil horizons from manual recovery (a) and drill recovery (b). Orange symbols = desert pavement; green symbols = playa. Grey shaded area indicates limit for 95% Confidence Intervals.

Figure 3. Non-metric multidimensional scaling (NMDS) ordination of Bray Curtis similarities for bacterial diversity versus soil depth from a) manual recovery, and b) drill recovery. Shaded areas indicate similarity clusters for soil communities at the same depth. The size of each symbol (circle or triangle) indicates Chao1 species richness index of the respective community.

Figure 4. Distribution of bacterial diversity with terrain and soil depth, for manual and drill-recovered samples. Coloured shading indicates relative abundance within each community for a given bacterial class. Absence of coloured shading indicates no recoverable bacteria. Asterisks indicate manually assisted drill sample recovery.

Soil microbial habitats in an extreme desert Mars-analogue environment

Methods

Field sites

A 50-km autonomous rover traverse along a natural elevational and climate gradient in the Atacama Desert was completed in 2013 (Fig 1). The western-most end of the transect (in the core hyperarid zone, S 24.76822', W 69.65134', 2053 m above sea level) included four sites situated at the southern foot of the Sierra Peñafiel mountains within alluvial plains between or on the slopes of isolated hills. The geological setting consists of volcanic rocks of Paleocene-Eocene age and detrital material eroded from surrounding outcrops that typified stony 'desert pavement' terrain habitat, comprised of surface soils mantled by gravels and bedrock debris. Three additional sites [S 24.63488', W 69.45375', 1984 m.a.s.l.] lie to the east at the edge of the Domeyko Cordillera range within a low-lying playa that has as its source the alluvial fans of the Sierra de Argomedo. At the transect's western end, regional climate is typical of the Atacama's hyperarid core, with mean annual rainfall of roughly 5-15 mm yr^{-1} and occasional fog incursion from the coast. At the eastern end, the playa sites occur within the topographical low and terminus for water runoff (snowmelt, rainfall) for the surrounding region, and thus these habitats receive significantly more moisture from easterly winter Andean precipitation and runoff than the desert pavement habitats to the west. In total, 133 samples were acquired (51 playa and 43 pavement), 42 samples were taken fully or semi-autonomously and 91 manually from soil pits. Of these, 85 samples were successfully processed with full geochemical and biological analyses.

*Robotic sample recov*ery

The Zöe rover built by the Robotics Institute at Carnegie Mellon University is a solar-powered rover designed to autonomously map and analyse contextual landscape and habitat visible and geochemical features (with on-board navigation cameras and Vis-NIR spectrometer on its mast) and to drill and deliver samples to on-board scientific instrumentation, including a Mars Micro-beam Raman Spectrometer (MMRS) [1]. The drill, developed by HoneyBee Robotics Corporation is a 15kg, 300 Watt, rotary-percussive and fully autonomous drill designed to capture powdered rocks and soil samples. The drill consists of a rotary-percussive drill head, sampling augur, brushing station, feed stage and deployment stage. using a vertical 19.1 mm diameter drill operating at 120 rpm, with the drill using a "bite" sampling approach where samples are captured in 10-20 cm intervals, to simulate Martian drilling scenario [2]. That is, after drilling 10-20 cm, the auger bit with the sample is pulled out of the hole, and the sample brushed off into a sample cup or sterile Whirlpak® (Nasco) bag. Initially autoclaved in the laboratory, the drill bit, brushing station, Z-stage and deployment stage were field sterilised with 70% ethanol prior to and after each site sampling. Aseptic techniques were also used throughout rover sampling operations, including minimal disturbance near the rover during all collections.

Manual Soil Pit Sampling

Post-drill, a soil pit adjacent to the drill hole was excavated manually. The pit wall was scraped using a plastic Sterileware® (Bel-Art Products) scoop or metal trowel sterilised with 70% ethanol. Samples from the soil pit were taken at surface (prior to excavation) to 800mm depths at 10-cm depth intervals. Samples were collected using aseptic techniques and tools using a Sterileware® (Bel-Art Products) sampling spatula or a stainless-steel spatula sterilised with 70% ethanol. Soil samples (50-200 g) were

collected from each depth layer for biology and geochemistry, with care taken to minimize mixing between different depths, and placed immediately into sterile falcon tubes or Whirlpak® (Nasco) bags. Deeper layers occasionally required a drill to obtain sample, and a Makita LXT drill was employed, with the drill bit first sterilised with 70% ethanol.

Soil geochemistry and microclimate data

On the rover, the Vis-NIR spectrometer and MMRS instruments collected real-time *in-situ* geochemical analyses of soil samples and these are reported in (Wei et al., 2013). In the laboratory, soil mineralogical and chemical analyses, including total carbon and total organic carbon (TOC), total nitrogen and available nitrogen (N), elemental compositions (Ca, K, Mg, Na, P, sulphate-S), pH, anion storage capacity, electrical conductivity (EC, a proxy for water availability, that is, more salt, less water, e.g. Crits-Cristoph et al., 2013), soluble salts and bulk density were measured according to standard soil chemical analysis methods[3].

Climate data were collected *in situ* (2013-2016) in soil pits at both a playa and desert site. However, following a record rainfall (85.5 mm) in 2015 the playa sensors could not be located. Meteorological monitoring included a mini-climate station (Onset H21-002) equipped with a leaf wetness smart sensor (Onset S-LWA-M003) to record soil surface conductivity as a proxy for the presence/absence of surficial water; and three soil volumetric moisture content probes (Onset S-SMC-M0005) placed at 10 cm, 30 cm and 80 cm depths. In addition, three soil relative humidity/temperature HOBO Pro v2 dataloggers (U23-002) were also placed at 10 cm, 30 cm and 80 cm. Data were recorded every 10-30 minutes from June 26 2013-Sept 20 2016. Gravimetric soil moisture content was obtained in the laboratory for comparison. Historical climate data were obtained

from regional observatories of the Chilean meteorological bureau and reference literature.

Environmental 16S rRNA gene-defined diversity

Total environmental genomic DNA were extracted from the soil samples using a modified CTAB method[4]. The extracted DNA were then adjusted, where possible, to 5 ng/μL before Illumina MiSeq library preparation as specified by the manufacturer (16S Metagenomic Sequencing Library Preparation Part # 15044223 Rev. B; Illumina, San Diego, CA, USA). Briefly, PCR was conducted with the primer set targeting the V3-V4 regions of bacterial and archaeal 16S rRNA gene: PCR1 forward (5′ TCGTCGGCAG CGTCAGATGT GTATAAGAGA CAGCCTACGG GNGGCWGCAG 3′) and PCR1 reverse (5′ GTCTCGTGGG CTCGGAGATG TGTATAAGAG ACAGGACTAC HVGGGTATCT AATCC 3′) with KAPA HiFi Hotstart Readymix (Kapa Biosystems, Wilmington, MA, USA) and the following thermocycling parameters: (1) 95°C for 3 min, (2) 25 cycles of 95°C for 30 s, 55°C for 30 s, 72°C for 30 s, 72°C for 5 min, and (3) holding the samples at 4°C. The amplicons were then indexed using Nextera XT index kit (Illumina). The indexed amplicons were purified and size selected using AMPure XP beads (Beckman-Coulter, Brea, CA, USA) before sequencing on an Illumina Miseq (Illumina) with the 500 cycle V2 chemistry (250 bp paired-end reads). A 5% PhiX spike-in was used, as per manufacturer's recommendation. The resulting raw sequencing data were then processed as previously described [5]. The R packages phyloseq[6], DESeq2[7] and ggplot2[8] were used for downstream analysis and visualisation including ordination and alpha diversity calculations. High-throughput sequencing of the 16S rRNA gene yielded 87,8875 quality filtered reads and 92 bacterial OTUs that were further analysed. All sequence data acquired during this investigation has been deposited in the NCBI GenBank under project accession number PRJEB22902.

Despite observing clear trends, recovery of genetic biosignatures also displayed considerable spatial heterogeneity/patchiness and this may explain, at least in part, why previous research has concluded some regions of the Atacama were microbiologically lifeless [9]. The patchiness of distribution for life in deserts [10] and extreme soils [11] are likely to be problematic in any study of extreme desert biota. We are confident, however, that our estimates provided a robust indication of endemic diversity. Our approach used a DNA recovery method that has been optimised for extreme desert soils and we employed positive and negative controls for all amplifications. We also adopted high coverage and carefully screened our sequence libraries for artefacts and contaminants. We also performed successful DNA extractions on pavement and playa soils that initially yielded negative extraction outcomes, after spiking these with *E.coli* from an axenic cell suspension in phosphate buffered saline solution at final cell concentrations of 10^3 – 10^7 cfu /g soil.

Statistical analysis

Linear Discriminant Analysis (LDA) of the geochemistry data (Online Supplementary Table S3) Of a total sample size of 62, n = 47 cases were used in estimation. Values below detection range were treated as 0. Cases containing missing values have been excluded. Null hypotheses: two-sided. For multiple comparisons correction, False Discovery Rate correction was applied simultaneously to the entire table. LDA was performed using the R package Flip Multivariates (https://github.com/Displayr/flipMultivariates). Canonical correspondence analysis (CCA) was performed with the R package vegan [12] to explore the strength of associations among the soil geochemistry profiles, bacterial taxa (OTUs) and site locations. Type III symmetrical scaling was used in the CCA plot, where both site and species scores both were scaled symmetrically by square root of eigenvalues. This

technique provided a weighted sum of the variables that maximizes the correlation between the canonical variates. A biplot was created to visualize the outcomes and help facilitate interpretation of the canonical variate scores. BEST analyses was conducted using the BIO-ENV procedure (Primer 7) to maximize the rank correlation between biotic and environmental data, thereby establishing a ranking ($_pw$) for the effects of environmental variables on diversity [13].

References

1. Tripathi, B. M. *et al.* Autonomous soil analysis by the Mars Micro-beam Raman Spectrometer (MMRS) on-board a rover in the Atacama Desert: A terrestrial test for planetary exploration. *Eukaryot. Cell* **46,** 1287–1297 (2017).
2. Zacny, K. *et al.* Life in the Atacama - The drill and sample delivery system. Results from the 2013 field campaign. in *Proceedings of the 45th Lunar and Planetary Science Conference* 1174 (2014).
3. Blakemore, L. C., Searle, P. L. & Daly, B. K. Methods for chemical analysis of soils. *NZ Soil Bur. Sci. Reports* **80** (1987).
4. Archer, S. D. J., McDonald, I. R., Herbold, C. W., Lee, C. K. & Cary, C. S. Benthic microbial communities of coastal terrestrial and ice shelf Antarctic meltwater ponds. *Frontiers in Microbiology* **6,** 485 (2015).
5. Maki, T. *et al.* Variations in the structure of airborne bacterial communities in Tsogt-Ovoo of Gobi desert area during dust events. *Air Qual. Atmos. Heal.* **10,** 249–260 (2017).
6. McMurdie, P. J. & Holmes, S. phyloseq: an R package for reproducible interactive analysis and graphics of microbiome census data. *PLoS One* **8,** e61217 (2013).
7. Love, M. I., Huber, W. & Anders, S. Moderated estimation of fold change and

dispersion for RNA-seq data with DESeq2. *Genome Biol.* **15,** 550 (2014).

8. Wickham, H. *ggplot2*. (Springer New York, 2009). doi:10.1007/978-0-387-98141-3

9. Navarro-Gonzalez, R. *et al.* Mars-like soils in the Atacama Desert, Chile, and the dry limit of microbial life. *Science* **302,** 1018–1021 (2003).

10. Rietkerk, M., Dekker, S. C., de Ruiter, P. C. & van de Koppel, J. Self-Organized Patchiness and Catastrophic Shifts in Ecosystems. *Science* **305,** 1926–1929 (2004).

11. Pointing, S. B. & Belnap, J. Microbial colonization and controls in dryland systems. *Nat. Rev. Microbiol.* **10,** 551–562 (2012).

12. Oksanen, J. *et al.* vegan: Community Ecology Package. *R package version 2.3-1* 264 (2015).

13. Clarke, K. & Gorley, R. Primer v7. 296p (2015).

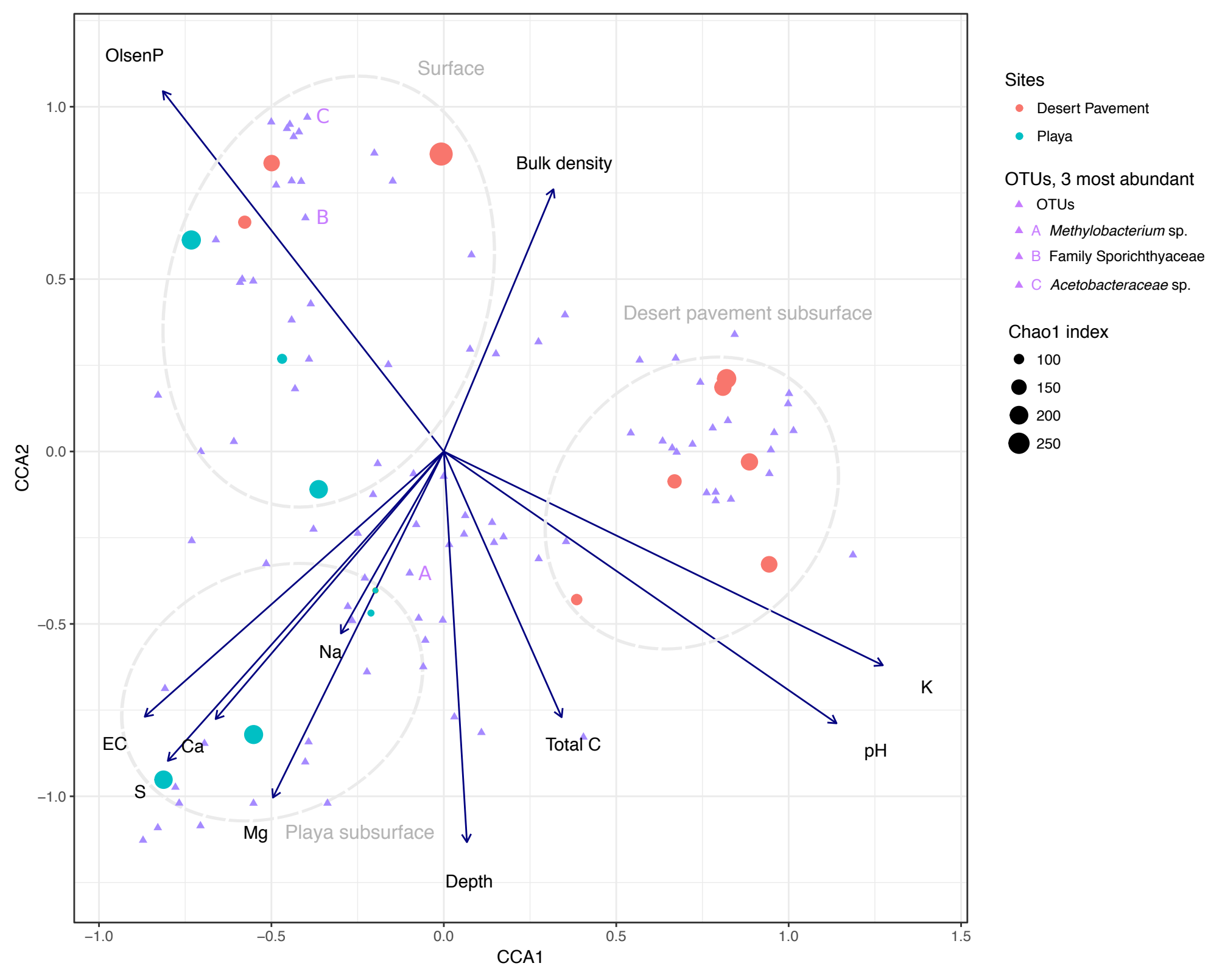
OlsenP
Surface
C
B
Bulk density
Desert pavement subsurface
A
Na
K
EC
Ca
S
Mg
Playa subsurface
Total C
pH
Depth
CCA1
CCA2
1.0
0.5
0.0
−0.5
−1.0
−1.0
−0.5
0.0
0.5
1.0
1.5
Sites
Desert Pavement
Playa
OTUs, 3 most abundant
OTUs
A Methylobacterium sp.
B Family Sporichthyaceae
C Acetobacteraceae sp.
Chao1 index
100
150
200
250

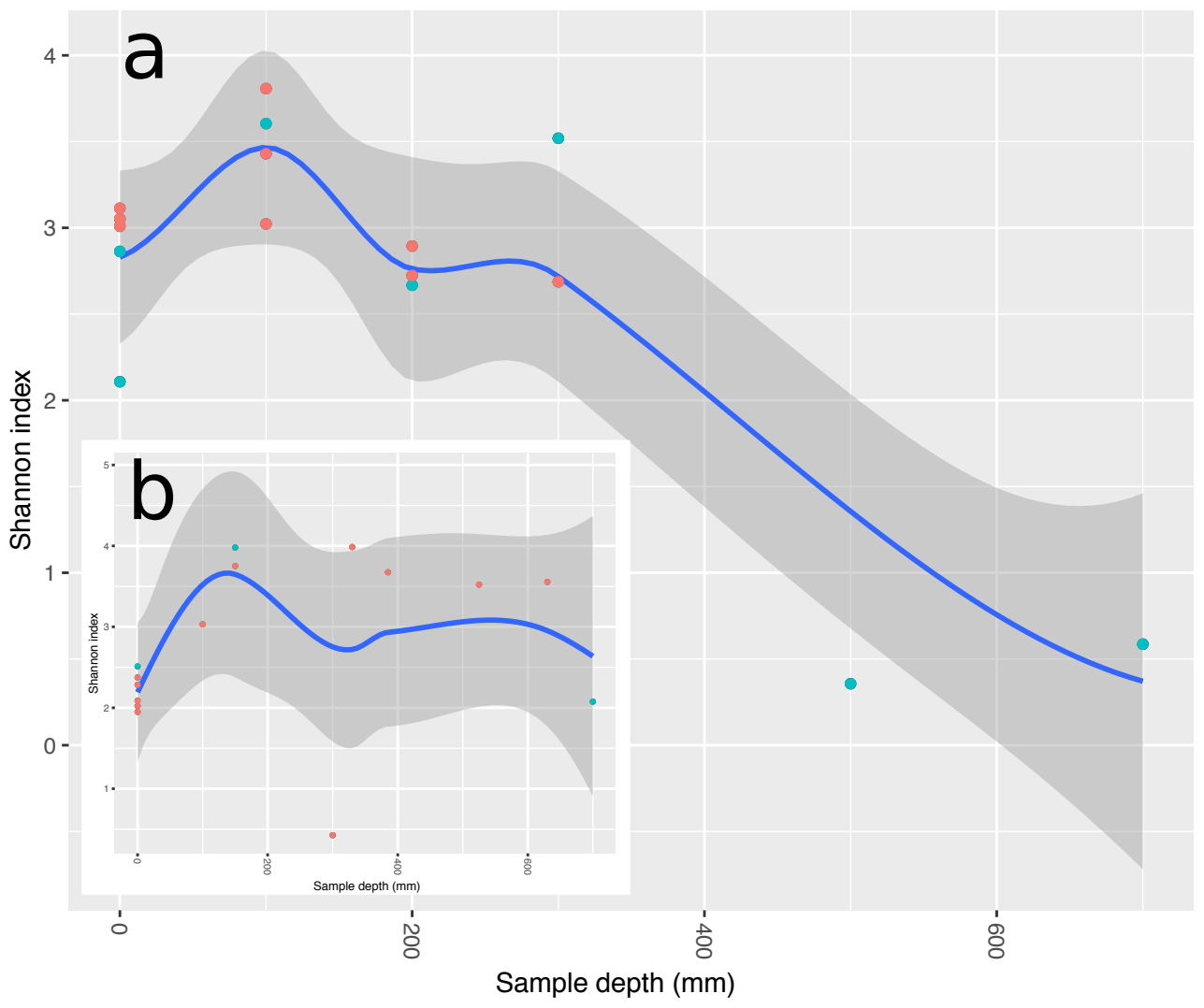
a
b
Shannon index
Sample depth (mm)
0
200
400
600
1
2
3
4

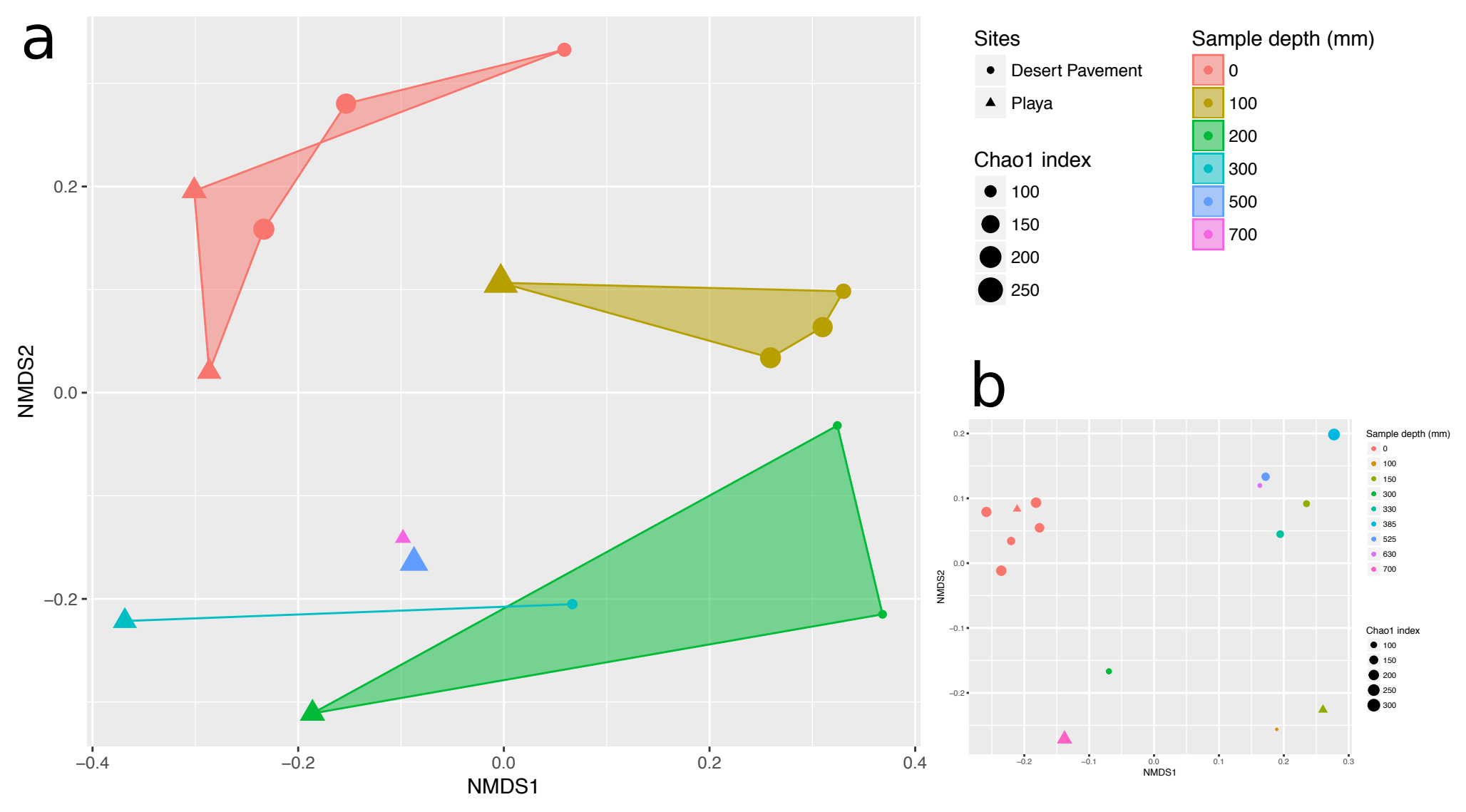
a
Sites
Desert Pavement
Playa
Chao1 index
100
150
200
250
Sample depth (mm)
0
100
200
300
500
700
NMDS2
NMDS1
0.2
0.0
−0.2
−0.4
−0.2
0.0
0.2
0.4
b
Sample depth (mm)
0
100
150
300
330
385
525
630
700
Chao1 index
100
150
200
250
300
NMDS2
NMDS1
0.2
0.1
0.0
−0.1
−0.2
−0.2
−0.1
0.0
0.1
0.2
0.3

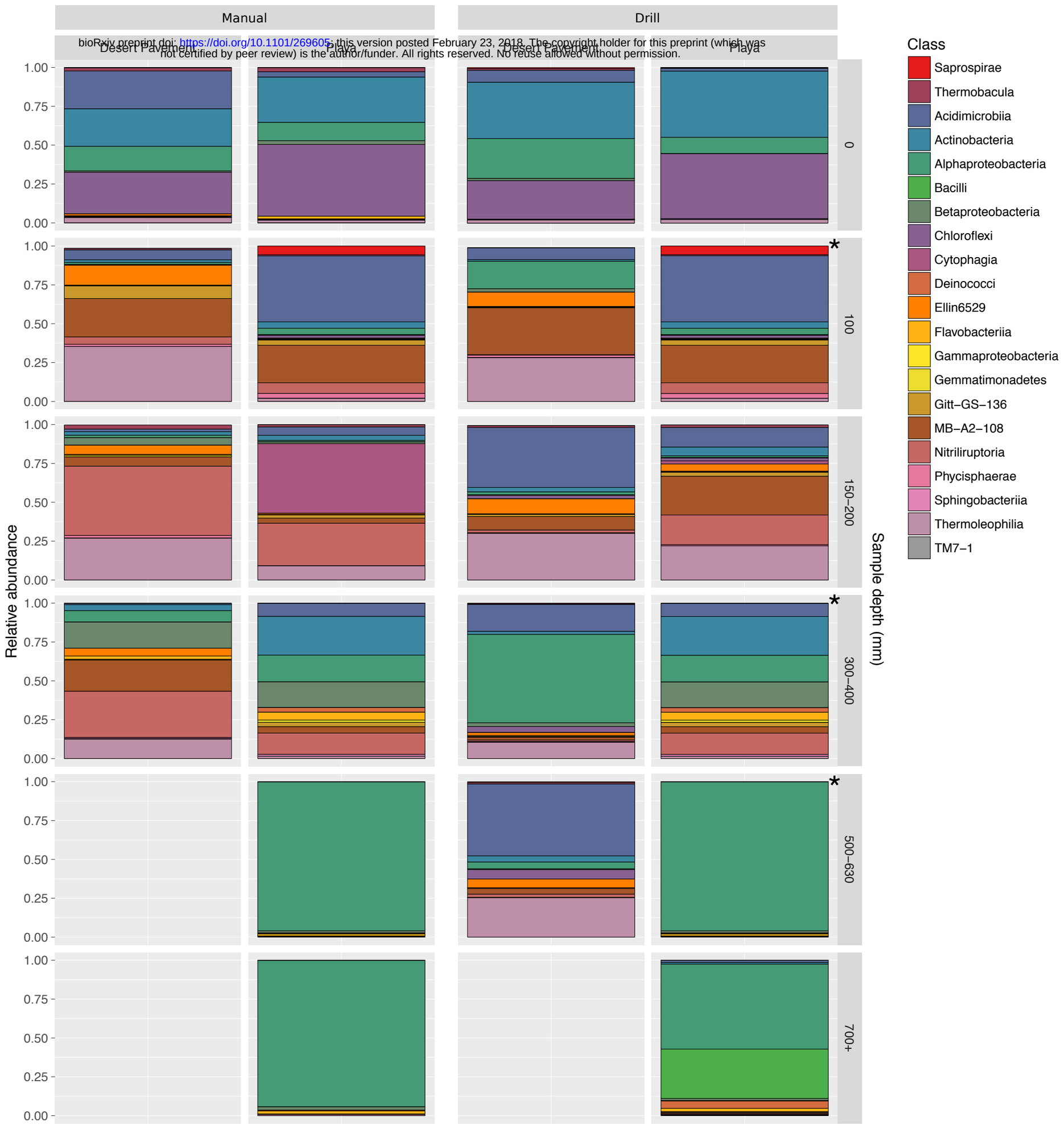

Soil microbial habitats in an extreme desert Mars-analogue environment
Online Supplementary Material

Figure S1. a) Sampling transect in the hyper-arid core of the Atacama Desert, circles along the transect line indicate location of sampling stations (transect line = 50km); b) Desert pavement terrain; c) Playa terrain; d) The Zöe rover; e) Rover drill apparatus; f) sample recovery from drill.

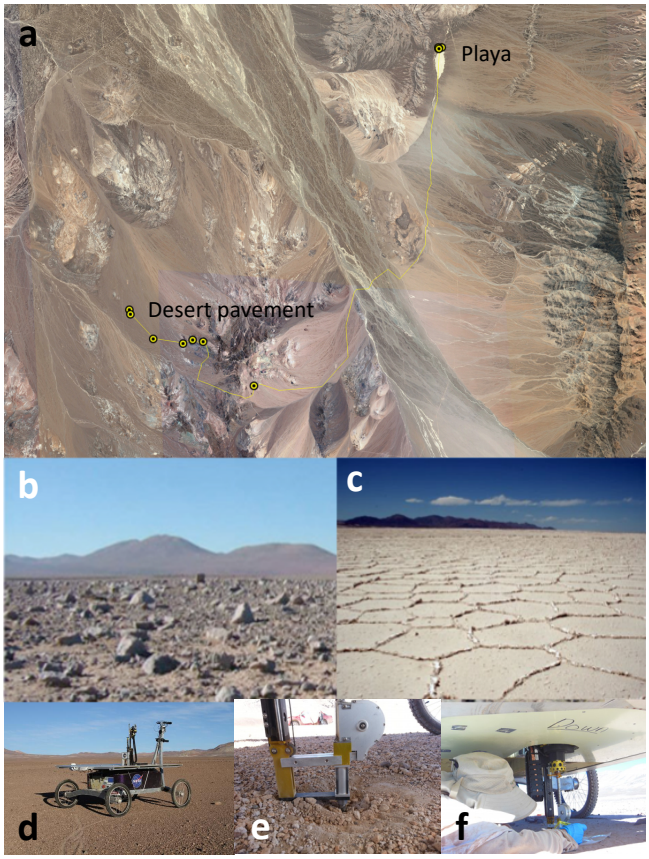

Figure S2. Trend in geochemical variables with depth, Orange symbols = desert pavement; green symbols = playa. Data for manually collected samples shown here. Trend lines were plotted using the Loess Method. Shaded area represents 95% confidence intervals.

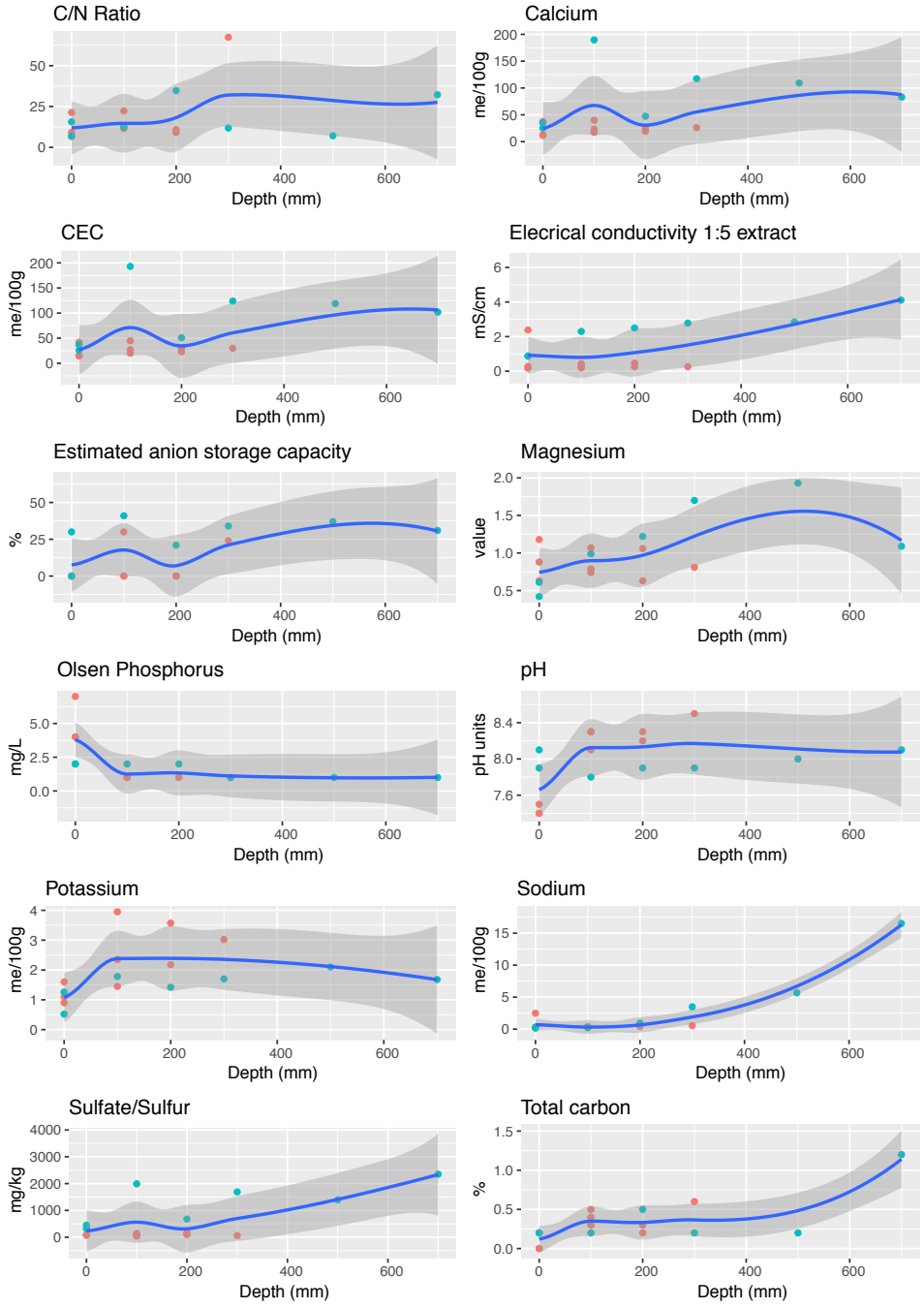

Figure S3. Summary plot of temporal variation in percent soil moisture, arrow denotes large stochastic rain event:

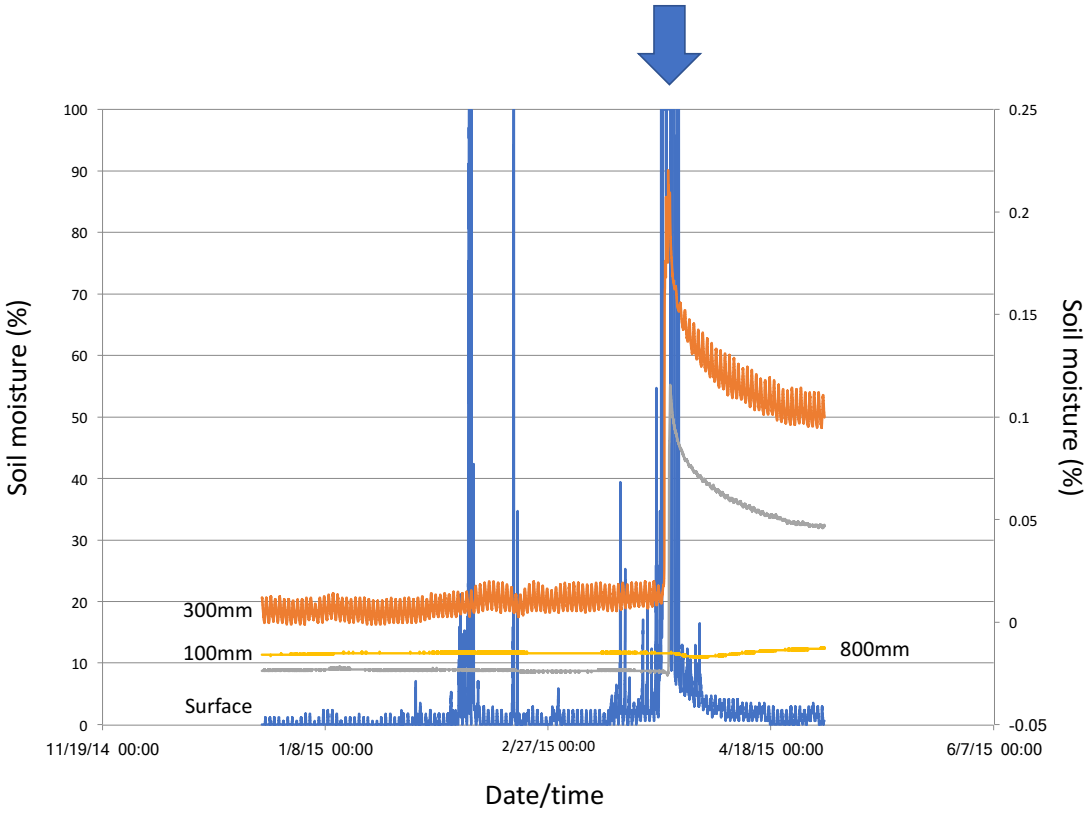

Figure S4. Combined NMDS ordination of Bray Curtis similarities for bacterial diversity indicated by Chao1 Index for desert pavement versus playa terrain. Ellipses represent 95% Confidence Interval for each grouping.

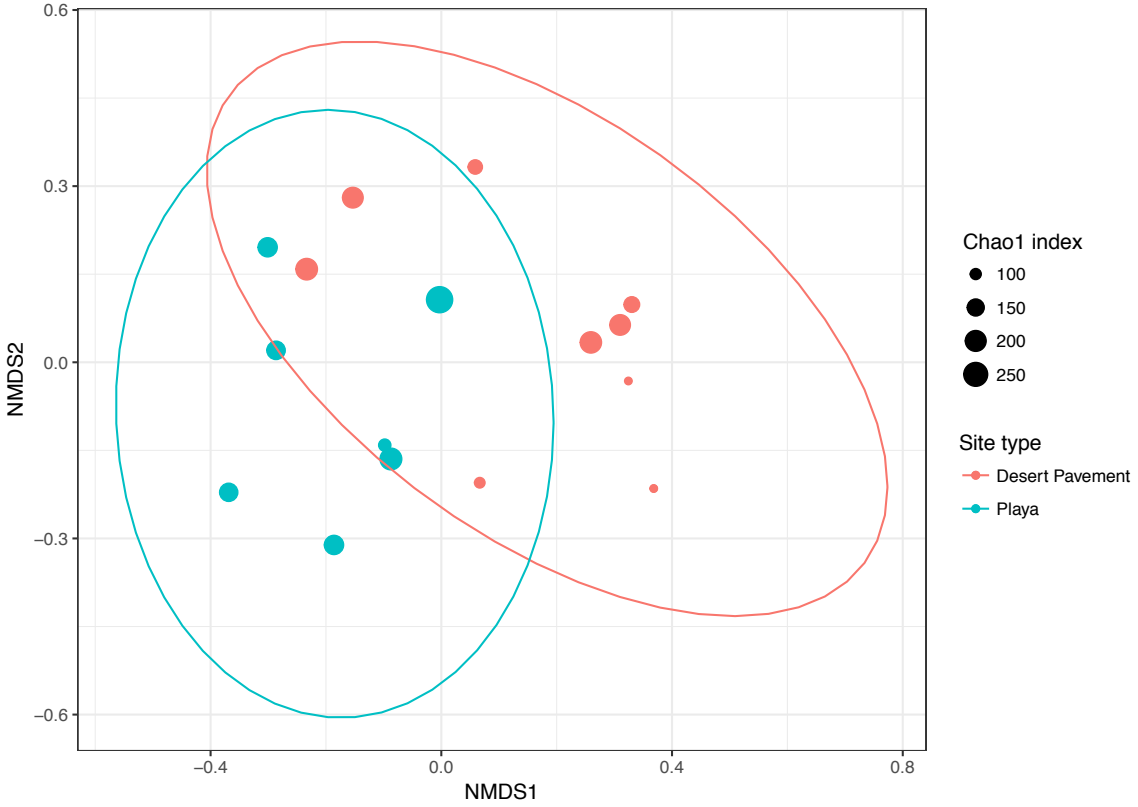

Figure S5. Bacterial 16S rRNA gene-defined diversity for all vertical soil horizons, showing stochastic occurrence of bacterial diversity at class level.

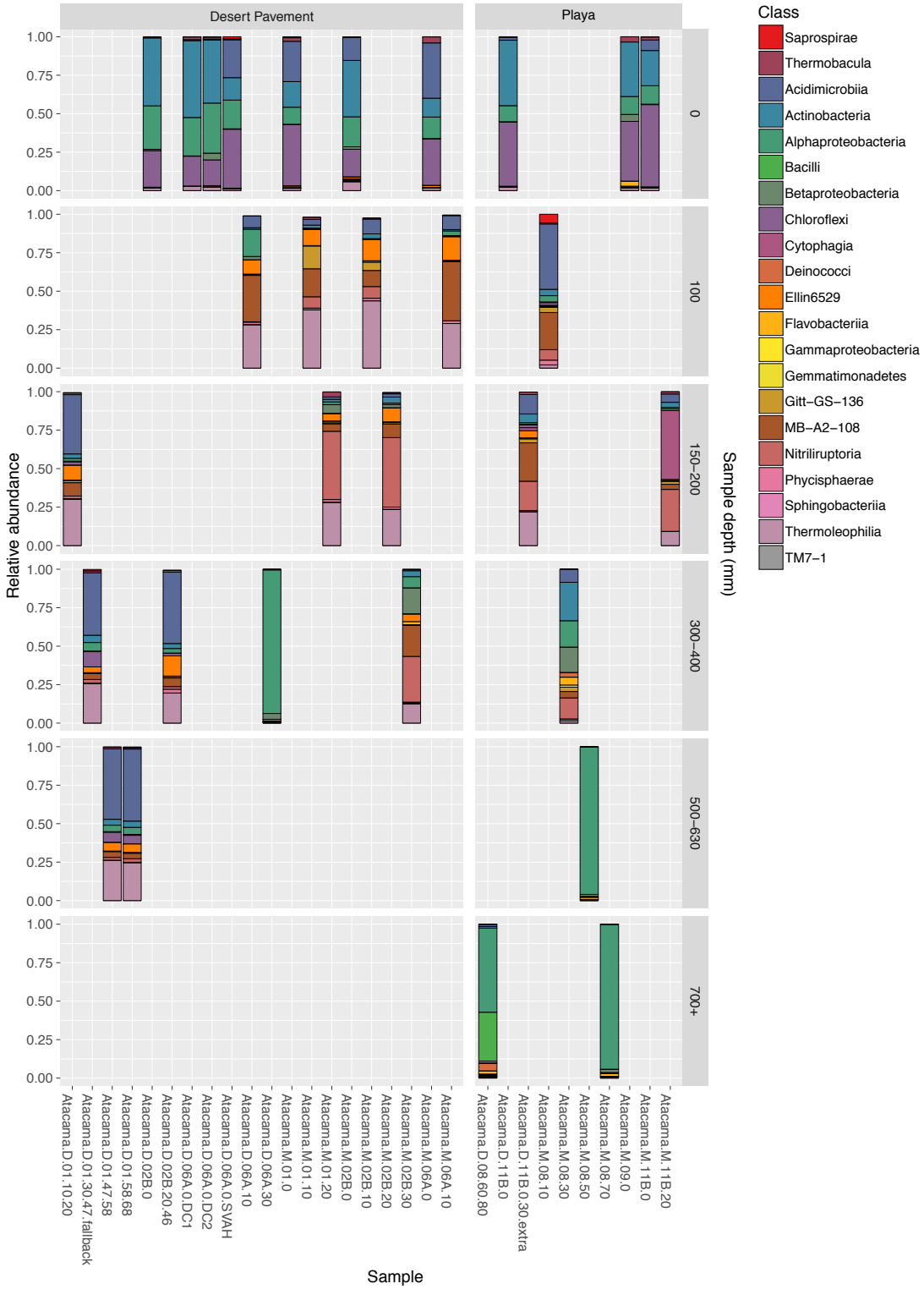

Table S1:

Summary of previous effort to detect biosignatures in Atacama soils

Early evidence suggested that challenging conditions in the Atacama might preclude recovery of microbial biosignatures such as environmental DNA from hyper-arid surface soil despite recovery of very low levels of cultivable bacterial strains from a bulk 0-10cm depth fraction [1]. Studies have reported low levels of cultivable strains from Atacama surface soil with widely varying estimates of diversity [1–4]. Some early success in recovering environmental DNA was achieved with relatively low-resolution analytical approaches such as fingerprinting and cloning: DNA fingerprinting studies the hyper-arid core soils (bulk 25-30cm depth) supported a limited and unique bacterial diversity dominated by *Gemmatimonadetes* and *Planctomycetes* phyla [5]. Clone library efforts suggested a different community dominated (>90%) by Actinobacteria of the genus *Frankia* in surface (bulk 0-1cm) and near surface (bulk 1-20cm) soil [3] and PLFA analysis has suggested the presence of Actinobacteria, Firmicutes and Proteobacteria as dominant phyla in Atacama soil [3,4].

The recent application of high-throughput sequencing has yielded more comprehensive diversity estimates, although these have also been restricted to surface and near-surface soil. An interrogation of soil from six locations in the Atacama Desert revealed that the hyper-arid core (0-15cm depth) displayed lowest diversity and taxa comprised approximately 80% Actinobacteria (Rubrobacterales, Actinomycetales, Acidimicrobiales) [6]. The study revealed significant correlation between air relative humidity and soil conductivity suggesting water availability and salt content of soil may be significant drivers of near-surface diversity [6]. Another high-throughput sequencing study of soil at the hyper-arid desert margin (bulk soil 15-25cm depth) indicated communities dominated by Actinobacteria and Chloroflexi, plus lower abundance of Acidobacteria and Proteobacteria [7]. These phyla are generally regarded as cosmopolitan desert soil taxa [8–11].

The different sampling approaches and diversity estimation methodologies used in previous studies makes comparison difficult, the cultivation studies yielded highly variable data not consistent with environmental DNA sequencing results, and the cultivation approach may not reflect abundant or dominant taxa within the community. The high-throughput sequencing data probably provide the most reliable estimates to date. These studies, however, have not addressed the issue of how microbial diversity may vary spatially with terrain, or within a soil depth horizon and with soil geochemistry, although this is critical to understanding desert soil geobiology as well as informing the most appropriate depth at which to search for life on Mars [12].

References

1. Navarro-Gonzalez, R. *et al.* Mars-like soils in the Atacama Desert, Chile, and the dry limit of microbial life. *Science* **302,** 1018–1021 (2003).
2. Okoro, C. K. *et al.* Diversity of culturable actinomycetes in hyper-arid soils of the Atacama Desert, Chile. *Antonie Van Leeuwenhoek* **95,** 121–133 (2009).
3. Connon, S. S. A., Lester, E. D. E., Shafaat, H. H. S., Obenhuber, D. C. & Ponce, A. Bacterial diversity in hyperarid Atacama Desert soils. *J Geophys Res - Biogeosci* **112,** G04S17 (2007).
4. Lester, E. D., Satomi, M. & Ponce, A. Microflora of extreme arid Atacama Desert soils. *Soil Biol. Biochem.* **39,** 704–708 (2007).
5. Drees, K. P. *et al.* Bacterial community structure in the hyperarid core of the

Atacama Desert, Chile. *Appl Env. Microbiol* **72,** 7902–7908 (2006).
6. Crits-Christoph, A. *et al.* Colonization patterns of soil microbial communities in the Atacama Desert. *Microbiome* **1,** 28 (2013).
7. Neilson, J. W. *et al.* Life at the hyperarid margin: novel bacterial diversity in arid soils of the Atacama Desert, Chile. *Extremophiles* **16,** 553–566 (2012).
8. Pointing, S. B. *et al.* Highly specialized microbial diversity in hyper-arid polar desert. *Proc. Natl. Acad. Sci. U.S.A.* **106,** 19964–19969 (2009).
9. Lee, K. C. *et al.* Niche Filtering of Bacteria in Soil and Rock Habitats of the Colorado Plateau Desert, Utah, USA. *Front. Microbiol.* **7,** 1489 (2016).
10. Stomeo, F. *et al.* Hypolithic and soil microbial community assembly along an aridity gradient in the Namib Desert. *Extremophiles* **17,** 329–337 (2013).
11. Chanal, A. *et al.* The desert of Tataouine: an extreme environment that hosts a wide diversity of microorganisms and radiotolerant bacteria. *Env. Microbiol* **8,** 514–525 (2006).
12. Fairen, A. *et al.* Astrobiology through the Ages of Mars: The Study of Terrestrial Analogues to Understand the Habitability of Mars. *Astrobiology* **10,** 821–843 (2010).

Table S2. Soil gravimetric moisture (a) and microclimate variables from in situ dataloggers (b) for selected soil horizons (data shown for ground-truthing soil pits).

a) Gravimetric soil moisture summary shown by habitat and depth.

Soil moisture (1.5 yrs post-2015 rain)	Site 01- desert pavement (%)	Site 08 – playa (%)
0 cm	0.12	2.3
10 cm	1.7	10.1
20 cm	1.2	8.8
30 cm	2.0	13.5
40 cm	3.5	15.0
50 cm	3.5	16.6
80 cm	2.2	8.7

b) Annual climate summary for Site 01 (June 2013-2014). A single rainfall event occurred May 24 2014 (Site 08 dataloggers were destroyed during a stochastic storm event).

	10 cm	**30 cm**	**80 cm**
Average Temp °C	19.9	20.3	20.9
Max Temp °C	34.4	26.1	25.3
Min Temp °C	3.2	14.7	20.0
Average %RH	22.6	20.4	22.6
Max %RH	97.7	31.2	23.6
Min %RH	9.8	16.8	20.9
#hrs liquid water from rain event	**304**	**0**	**0**

Table S3. Soil geochemistry variables for desert pavement and playa soil horizons. Asterisks indicate samples that yielded environmental DNA sequences.

Sample Name	Site	Site Type	Soil depth	pH	Olsen Phosphorus	Anion Storage Capacity (estimated)	Sulphate Sulphur	Extractable Organic Sulphur	Available Nitrogen (15cm Depth)	Anaerobically Mineralisable N	Anaerobically Mineralisable N/Total N Ratio	Organic Matter	Total Carbon	Total Nitrogen	C/N Ratio	Soluble Salts (Field)	EC (in 1:5 Extract)	Potassium	Calcium	Magnesium	Sodium	Potassium	Calcium	Magnesium	Sodium	CEC	Total Base Saturation	Volume Weight
			cm	pH Units	mg/L	%	mg/kg	mg/kg	kg/ha	µg/g	%	%	%	%		%	mS/cm	me/100g	me/100g	me/100g	me/100g	%BS	%BS	%BS	%BS	me/100g	%	g/mL
Atacama.M.01.0*	01	Desert Pavement	0	7.5	4	< 15	88	< 2	12	6	12.6	< 0.2	< 0.1	< 0.04	9.2	0.1	0.28	0.9	12.8	0.88	0.29	6	86	5.9	2	15	100	1.27
Atacama.M.01.10*	01	Desert Pavement	10	8.3	1	< 15	43	< 2	< 10	< 5	2.3	0.5	0.3	< 0.04	22.3	0.07	0.19	2.35	23.2	0.79	0.39	8.8	87	2.9	1.4	27	100	1.26
Atacama.M.01.20*	01	Desert Pavement	20	8.3	1	< 15	99	< 2	< 10	< 5	0.6	0.5	0.3	< 0.04	9	0.09	0.25	3.57	25.2	1.06	0.66	11.7	83	3.5	2.2	30	100	1.29
Atacama.M.01.30	01	Desert Pavement	30	7.9	< 1	-	-	-	< 10	< 5	0.9	0.8	0.4	< 0.04	40.9	0.81	2.32	2.75	158.6	0.9	0.65	1.7	97	0.6	0.4	163	100	1.26
Atacama.M.01.40	01	Desert Pavement	40	7.7	< 1	-	-	-	-	-	-	0.3	0.2	< 0.04	33.7	0.83	2.37	2.25	191.4	0.82	0.94	1.2	98	0.4	0.5	195	100	1.41
Atacama.M.01.50	01	Desert Pavement	50	7.5	2	-	-	-	10	5	0.8	1.8	1	0.06	16.2	1.03	2.94	2.42	172.4	0.53	4.34	1.3	96	0.3	2.4	180	100	1.34
Atacama.M.01.60	01	Desert Pavement	60	7.9	< 1	-	-	-	< 10	< 5	< 0.5	< 0.2	< 0.1	< 0.04	3.4	1.35	3.86	2.96	193	0.66	6.26	1.5	95	0.3	3.1	203	100	1.46
Atacama.M.01.70	01	Desert Pavement	70	8.2	1	-	-	-	< 10	< 5	< 0.5	< 0.2	0.1	< 0.04	3	1.32	3.77	3.17	204	0.68	7.5	1.5	95	0.3	3.5	215	100	1.44
Atacama.M.01.80	01	Desert Pavement	80	8.1	1	-	-	-	< 10	< 5	< 0.5	0.3	0.2	0.06	3	1.51	4.31	3.07	139	0.51	12.08	2	90	0.3	7.8	155	100	1.48
Atacama.M.28.0*	2B	Desert Pavement	0	7.4	4	-	-	-	12	6	5	0.4	0.2	< 0.04	21.3	0.83	2.38	1.6	37.3	0.63	2.48	3.8	89	1.5	5.9	42	100	1.49
Atacama.M.28.10*	2B	Desert Pavement	10	8.3	1	< 15	69	< 2	< 10	< 5	< 0.5	0.7	0.4	< 0.04	12.6	0.09	0.27	1.45	17.3	0.74	0.28	7.3	87	3.7	1.4	20	100	1.12
Atacama.M.28.20*	2B	Desert Pavement	20	8.2	1	< 15	170	< 2	< 10	< 5	0.9	0.4	0.2	< 0.04	10.8	0.16	0.47	2.18	19.3	0.63	0.39	9.7	86	2.8	1.7	23	100	1.37
Atacama.M.28.30*	2B	Desert Pavement	30	8.5	1	24	62	< 2	< 10	< 5	1	1	0.6	< 0.04	67.4	0.09	0.26	3.02	26	0.81	0.55	9.9	86	2.7	1.8	30	100	1.34
Atacama.M.28.40	2B	Desert Pavement	40	7.9	< 1	-	0	-	< 10	< 5	1.1	0.7	0.4	< 0.04	40.4	0.62	1.78	3.06	29.6	1.33	1.21	8.7	84	3.8	3.5	35	100	1.55
Atacama.M.28.50	2B	Desert Pavement	50	8.1	1	-	0	-	-	-	-	0.5	0.3	< 0.04	37.9	0.52	1.48	2.45	24	1.11	2.97	8	79	3.6	9.7	31	100	1.48
Atacama.M.28.60	2B	Desert Pavement	60	8.4	1	-	0	-	-	-	-	0.8	0.5	< 0.04	28.3	-	-	2.86	29.3	0.6	8.5	6.9	71	1.4	20.6	41	100	1.53
Atacama.M.28.70	2B	Desert Pavement	70	8.3	< 1	< 15	1,321	< 2	< 10	< 5	< 0.5	0.5	0.3	< 0.04	18.8	1.06	3.03	2.9	92.3	0.44	10.62	2.7	87	0.4	10	106	100	1.49
Atacama.M.28.80	2B	Desert Pavement	80	7.7	< 1	< 15	2,060	< 2	< 10	< 5	< 0.5	0.2	0.1	0.04	3.2	1.1	3.14	2.55	220	0.63	3.57	1.1	97	0.3	1.6	226	100	1.32
Atacama.M.06.0*	6A	Desert Pavement	0	7.4	7	< 15	74	< 2	15	7	9.8	< 0.2	< 0.1	< 0.04	6.7	0.06	0.17	1.1	11.5	1.18	0.24	7.5	78	8	1.6	15	95	1.42
Atacama.M.06.10*	6A	Desert Pavement	10	8.1	1	30	141	5	< 10	< 5	< 0.5	0.9	0.5	0.05	11.5	0.15	0.43	3.95	39.8	1.07	0.4	8.7	88	2.4	0.9	45	100	1.22
Atacama.M.06.20	6A	Desert Pavement	20	7.8	1	-	0	-	< 10	< 5	2.1	1.1	0.6	< 0.04	44.9	0.88	2.51	7.33	153.4	1.2	0.62	4.5	94	0.7	0.4	163	100	1.29
Atacama.M.06.30	6A	Desert Pavement	30	7.8	1	-	0	-	-	-	-	0.7	0.4	< 0.04	29.1	-	-	7.07	68	0.57	0.81	9.3	89	0.7	1.1	76	100	1.46
Atacama.M.06.40	6A	Desert Pavement	40	8.2	2	-	0	-	< 10	< 5	< 0.5	< 0.2	< 0.1	< 0.04	1.9	1.38	3.95	5.14	153.1	0.86	12.91	3	89	0.5	7.5	172	100	1.29
Atacama.M.06.50	6A	Desert Pavement	50	8.7	< 1	< 15	1,467	< 2	< 10	< 5	< 0.5	< 0.2	< 0.1	0.05	0.8	1.19	3.39	4.8	22.3	0.31	19.29	10.3	48	0.7	41.3	47	100	1.48
Atacama.M.06.80	6A	Desert Pavement	80	8.2	1	-	0	-	-	-	-	0.2	0.1	0.26	0.5	-	-	4.74	131.4	0.98	37	2.7	75	0.6	21.2	174	100	1.33
Atacama.M.08.0	08	Playa	0	7.8	4	43	1,940	< 2	< 10	< 5	2.8	0.4	0.2	< 0.04	13.6	0.79	2.26	0.76	119.9	0.39	0.24	0.6	99	0.3	0.2	121	100	0.99
Atacama.M.08.10*	08	Playa	10	7.8	2	41	1,992	< 2	< 10	< 5	0.9	0.4	0.2	< 0.04	12.4	0.8	2.3	1.78	189.7	0.99	0.22	0.9	98	0.5	0.1	193	100	0.89
Atacama.M.08.20	08	Playa	20	8	2	39	1,131	< 2	< 10	< 5	1.1	0.3	0.2	< 0.04	9.6	0.85	2.43	2.56	77.6	2.33	1.37	3.1	93	2.8	1.6	84	100	0.96
Atacama.M.08.30*	08	Playa	30	7.9	1	34	1,690	< 2	< 10	< 5	2	0.4	0.2	< 0.04	11.8	0.97	2.78	1.7	117.3	1.7	3.49	1.4	94	1.4	2.8	124	100	1.12
Atacama.M.08.40	08	Playa	40	7.9	2	35	949	< 2	< 10	< 5	1.4	0.4	0.2	< 0.04	6.5	0.97	2.78	1.91	87.1	1.62	3.75	2	92	1.7	4	94	100	1.04
Atacama.M.08.50*	08	Playa	50	8	1	37	1,393	< 2	10	7	2.5	0.4	0.2	< 0.04	7.1	1	2.85	2.1	109.3	1.93	5.69	1.8	92	1.6	4.8	119	100	0.98
Atacama.M.08.60	08	Playa	60	8	1	29	1,766	< 2	10	7	2.2	0.4	0.2	< 0.04	6.5	1.15	3.29	1.89	105.7	1.34	9.28	1.6	89	1.1	7.9	118	100	0.95
Atacama.M.08.70*	08	Playa	70	8.1	1	31	2,350	< 2	< 10	6	1.6	2.1	1.2	< 0.04	32.2	1.44	4.11	1.68	83	1.09	16.51	1.6	81	1.1	16.1	102	100	0.96
Atacama.M.08.80	08	Playa	80	8.4	1	16	2,370	< 2	< 10	< 5	< 0.5	0.2	0.1	< 0.04	5.4	1.5	4.28	0.91	108.8	0.22	18.04	0.7	85	< 0.2	14.1	128	100	1.2
Atacama.M.09.0*	09	Playa	0	7.9	2	< 15	449	< 2	< 10	< 5	1.8	0.3	0.2	< 0.04	15.6	0.31	0.88	0.52	25.1	0.42	0.3	2	95	1.6	1.1	26	100	1.41
Atacama.M.09.10	09	Playa	10	7.8	< 1	< 15	1,018	< 2	< 10	< 5	2	0.3	0.2	< 0.04	22.1	0.76	2.17	0.25	64.9	0.1	0.06	0.4	99	< 0.2	< 0.1	65	100	1.46
Atacama.M.09.20	09	Playa	20	7.9	2	21	1,478	< 2	< 10	< 5	< 0.5	0.4	0.2	< 0.04	11	0.8	2.28	1.51	134.6	0.84	0.23	1.1	98	0.6	0.2	137	100	1.07
Atacama.M.09.30	09	Playa	30	7.8	< 1	< 15	1,226	57	< 10	< 5	< 0.5	0.3	0.2	< 0.04	12.7	0.78	2.24	0.48	91.2	0.67	0.22	0.5	99	0.7	0.2	93	100	1.41
Atacama.M.09.40	09	Playa	40	8	1	< 15	1,338	103	< 10	< 5	< 0.5	0.3	0.2	< 0.04	25.1	0.9	2.56	0.76	181.1	0.58	1.49	0.4	98	0.3	0.8	184	100	1.22
Atacama.M.09.50	09	Playa	50	8	< 1	34	1,329	< 2	21	14	5.2	0.4	0.2	< 0.04	7.9	0.91	2.59	1.97	144.3	1.6	1.68	1.3	96	1.1	1.1	150	100	0.99
Atacama.M.09.60	09	Playa	60	7.8	< 1	< 15	1,036	< 2	< 10	< 5	< 0.5	0.3	0.2	< 0.04	22.8	0.79	2.26	0.53	58.5	0.39	0.45	0.9	98	0.6	0.7	60	100	1.48
Atacama.M.09.70	09	Playa	70	7.7	< 1	< 15	1,508	< 2	< 10	< 5	0.5	0.3	0.2	< 0.04	14.9	0.81	2.32	0.77	94.5	0.65	0.69	0.8	98	0.7	0.7	97	100	1.23
Atacama.M.09.80	09	Playa	80	7.6	< 1	< 15	1,145	16	< 10	< 5	1	0.2	0.1	< 0.04	7.2	0.79	2.25	0.45	102.6	0.37	0.42	0.4	99	0.4	0.4	104	100	1.48
Atacama.M.10.0	10	Playa	0	7.8	3	32	2,210	< 2	< 10	< 5	3	0.3	0.1	< 0.04	10.6	0.82	2.35	0.62	177.2	0.23	0.87	0.3	99	< 0.2	0.5	179	100	0.96
Atacama.M.10.10	10	Playa	10	7.8	< 1	< 15	1,485	8	< 10	< 5	1.7	0.6	0.3	< 0.04	30.5	0.8	2.29	1.34	261	0.39	0.18	0.5	99	< 0.2	< 0.1	263	100	1.08
Atacama.M.10.20	10	Playa	20	7.7	< 1	< 15	1,930	< 2	< 10	< 5	< 0.5	0.2	0.1	< 0.04	9.5	0.86	2.45	3.4	231	0.75	0.33	1.4	98	0.3	0.1	235	100	1.17
Atacama.M.10.30	10	Playa	30	8.5	< 1	45	3,330	146	< 10	< 5	< 0.5	0.4	0.2	< 0.04	14.7	2.12	6.07	8.13	226	1.02	18.59	3.2	89	0.4	7.3	254	100	1.11
Atacama.M.10.40	10	Playa	40	8.6	< 1	39	3,890	4	< 10	< 5	< 0.5	0.2	0.1	0.07	1.8	3.29	9.4	2.79	200	0.9	36.2	1.2	83	0.4	15.1	240	100	1.25
Atacama.M.10.50	10	Playa	50	8.1	< 1	32	2,930	132	< 10	< 5	< 0.5	0.2	0.1	0.46	< 0.5	5.42	15.49	2.6	185.5	0.62	69.3	1	72	0.2	26.8	258	100	1.16
Atacama.M.10.60	10	Playa	60	8.1	< 1	27	2,110	< 2	< 10	< 5	< 0.5	< 0.2	< 0.1	0.21	< 0.5	3.38	9.66	1.84	119.4	0.56	41.4	1.1	73	0.3	25.3	163	100	1.21
Atacama.M.10.70	10	Playa	70	8	< 1	30	2,770	< 2	< 10	< 5	< 0.5	< 0.2	< 0.1	0.05	0.7	3.09	8.82	2.26	159.7	0.56	29.1	1.2	83	0.3	15.2	192	100	1.07
Atacama.M.10.80	10	Playa	80	8	1	< 15	2,400	134	< 10	< 5	< 0.5	0.2	0.1	0.17	0.8	3.06	8.75	1.83	225	0.45	30.7	0.7	87	< 0.2	11.9	258	100	1.14
Atacama.M.11B.0*	11B	Playa	0	8.1	2	30	321	< 2	< 10	< 5	0.7	0.4	0.2	< 0.04	6.8	0.3	0.87	1.26	34.8	0.61	0.17	3.4	94	1.7	0.5	37	100	1.17
Atacama.M.11B.10	11B	Playa	10	7.9	1	19	916	< 2	< 10	< 5	0.5	0.3	0.2	< 0.04	10.3	0.82	2.33	1.39	61	0.58	0.42	2.2	96	0.9	0.7	63	100	1.13
Atacama.M.11B.20	11B	Playa	20	7.9	2	21	676	< 2	< 10	< 5	1	0.8	0.5	< 0.04	34.7	0.88	2.5	1.42	47.3	1.22	0.95	2.8	93	2.4	1.9	51	100	1.24
Atacama.M.11B.30	11B	Playa	30	8	< 1	18	1,266	< 2	< 10	< 5	1	0.2	0.1	< 0.04	5.6	1.04	2.98	1.3	54.3	1.51	5.83	2.1	86	2.4	9.3	63	100	1.29
Atacama.M.11B.40	11B	Playa	40	7.8	< 1	< 15	1,082	< 2	< 10	< 5	1.5	< 0.2	< 0.1	< 0.04	3.3	0.99	2.83	0.56	27.2	0.81	4.01	1.7	83	2.5	12.3	33	100	1.41
Atacama.M.11B.50	11B	Playa	50	7.9	1	< 15	633	< 2	< 10	< 5	< 0.5	0.2	0.1	< 0.04	4	0.91	2.61	1.17	53.9	0.73	0.86	2.1	95	1.3	1.5	57	100	1.2
Atacama.M.11B.60	11B	Playa	60	7.9	< 1	< 15	473	< 2	< 10	< 5	< 0.5	< 0.2	< 0.1	< 0.04	6.1	0.61	1.74	0.78	26.3	0.67	0.6	2.7	93	2.4	2.1	28	100	1.35
Atacama.M.11B.70	11B	Playa	70	8.1	< 1	< 15	543	< 2	< 10	< 5	< 0.5	< 0.2	< 0.1	< 0.04	7.2	0.72	2.05	0.92	32.1	0.78	1.26	2.6	92	2.2	3.6	35	100	1.26
Atacama.M.11B.80	11B	Playa	80	7.9	< 1	< 15	943	< 2	< 10	< 5	1.8	< 0.2	< 0.1	< 0.04	8.1	0.75	2.15	0.33	32.9	0.23	0.85	0.9	96	0.7	2.5	34	100	1.57

Table S4. Environmental DNA recovery from desert pavement and playa soil horizons.

Sample ID	Collection	Site Type	Sample depth (cm)	Site	DNA ng/g
AT13-01 surface	Manual	Desert Pavement	Surface	01	3.56
AT13-01 10cm	Manual	Desert Pavement	10	01	3.08
AT13-01 20cm	Manual	Desert Pavement	20	01	<0.067
AT13-01 30cm	Manual	Desert Pavement	30	01	<0.067
AT13-01 40cm	Manual	Desert Pavement	40	01	<0.067
AT13-01 50cm	Manual	Desert Pavement	50	01	<0.067
AT13-01 60cm	Manual	Desert Pavement	60	01	<0.067
AT13-01 70cm	Manual	Desert Pavement	70	01	<0.067
AT13-01 80cm	Manual	Desert Pavement	80	01	<0.067
AT13-02B surface	Manual	Desert Pavement	Surface	02	<0.067
AT13-02B 10cm	Manual	Desert Pavement	10	02	3.28
AT13-02B 20cm	Manual	Desert Pavement	20	02	<0.067
AT13-02B 30cm	Manual	Desert Pavement	30	02	<0.067
AT13-02B 40cm	Manual	Desert Pavement	40	02	<0.067
AT13-02B 50cm	Manual	Desert Pavement	50	02	<0.067
AT13-02B 60cm	Manual	Desert Pavement	60	02	<0.067
AT13-02B 70cm	Manual	Desert Pavement	70	02	<0.067
AT13-02B 80cm	Manual	Desert Pavement	80	02	<0.067
AT13-06A surface	Manual	Desert Pavement	Surface	06	6.507
AT13-06A 10cm	Manual	Desert Pavement	10	06	1.083
AT13-06A 20cm	Manual	Desert Pavement	20	06	<0.067
AT13-06A 30cm	Manual	Desert Pavement	30	06	<0.067
AT13-06A 40cm	Manual	Desert Pavement	40	06	<0.067
AT13-06A 50cm	Manual	Desert Pavement	50	06	<0.067
AT13-06A 80cm	Manual	Desert Pavement	80	06	<0.067
AT13-08 10cm	Manual	Playa	10	08	0.661
AT13-08 20cm	Manual	Playa	20	08	0.597
AT13-08 30cm	Manual	Playa	30	08	<0.067

AT13-08 50cm	Manual	Playa	50	08	<0.067
AT13-08 70cm	Manual	Playa	70	08	<0.067
AT13-08 80cm	Manual	Playa	80	08	<0.067
AT13-09 surface	Manual	Playa	Surface	09	<0.067
AT13-09 10cm	Manual	Playa	10	09	0.368
AT13-09 30cm	Manual	Playa	30	09	<0.067
AT13-09 40cm	Manual	Playa	40	09	<0.067
AT13-09 60cm	Manual	Playa	60	09	<0.067
AT13-09 70cm	Manual	Playa	70	09	<0.067
AT13-10 20cm	Manual	Playa	20	10	0.581
AT13-10 30cm	Manual	Playa	30	10	<0.067
AT13-10 40cm	Manual	Playa	40	10	<0.067
AT13-10 50cm	Manual	Playa	50	10	<0.067
AT13-10 60cm	Manual	Playa	60	10	<0.067
AT13-10 80cm	Manual	Playa	80	10	<0.067
AT13-11B surface	Manual	Playa	Surface	11	<0.067
AT13-11B 10cm	Manual	Playa	10	11	0.837
AT13-11B 20cm	Manual	Playa	20	11	0.331
AT13-11B 30cm	Manual	Playa	30	11	0.485
AT13-11B 40cm	Manual	Playa	40	11	<0.067
AT13-11B 50cm	Manual	Playa	50	11	0.293
AT13-11B 60cm	Manual	Playa	60	11	<0.067
AT13-11B 70cm	Manual	Playa	70	11	0.315
AT13-11B 80cm	Manual	Playa	80	11	<0.067
AT13-01 10-20cm	Drill	Desert Pavement	10-20	01	0.315
AT13-01 30-47cm	Drill	Desert Pavement	30-47	01	4.667
AT13-01 47-58cm	Drill	Desert Pavement	47-58	01	0.312
AT13-01 58-68cm	Drill	Desert Pavement	58-68	01	0.789
AT13-01 68-77cm	Drill	Desert Pavement	68-77	01	<0.067
AT13-02B surface	Drill	Desert Pavement	Surface	02	<0.067
AT13-02B 20-46cm	Drill	Desert Pavement	20-46	02	6.4

AT13-06A 10cm	Drill	Desert Pavement	10	06	<0.067
AT13-06A 30cm	Drill	Desert Pavement	30	06	<0.067
AT13-06A 80cm	Drill	Desert Pavement	80	06	<0.067
AT13-06A	Drill	Desert Pavement	Surface	06	<0.067
AT13-06A Surface	Drill	Desert Pavement	Surface	06	<0.067
AT13-08 Surface	Drill	Playa	Surface	08	<0.067
AT13-08 17-30cm	Drill	Playa	17-30	08	<0.067
AT13-08 30-60cm	Drill	Playa	30-60	08	<0.067
AT13-08 60-80cm	Drill	Playa	60-80	08	<0.067
AT13-08 after 60-80cm	Drill	Playa	>60-80	08	<0.067
AT13-09 surface	Drill	Playa	Surface	09	<0.067
AT13-09 0-30cm	Drill	Playa	0-30	09	1.4
AT13-09 30-60cm	Drill	Playa	30-60	09	<0.067
AT13-10 surface	Drill	Playa	Surface	10	<0.067
AT13-10 10-30cm	Drill	Playa	10-30	10	<0.067
AT13-10 24-71cm	Drill	Playa	24-71	10	0.315
AT13-10 0-24cm extra	Drill	Playa	0-24	10	<0.067
AT13-10 0-30cm extra	Drill	Playa	0-30	10	<0.067
AT13-10 40-80cm	Drill	Playa	40-80	10	<0.067
AT13-11B surface	Drill	Playa	Surface	11	<0.067
AT13-11B 0-10cm	Drill	Playa	0-10	11	<0.067
AT13-11B 10-30cm	Drill	Playa	10-30	11	0.629
AT13-11B 33-63cm	Drill	Playa	33-63	11	<0.067
AT13-11B 0-30cm extra	Drill	Playa	0-30	11	0.597
AT13-11B 77-80cm	Drill	Playa	77-80	11	0.277
AT13-11B 0-55cm extra	Drill	Playa	0-55	11	0.848